

Synthesis of hollow Mn_3O_4 -in- Co_3O_4 magnetic microspheres and its chemiluminescence and catalytic properties

Fei Teng ^{a,*}, Tongguang Xu ^b, Shuhui Liang ^b, Gauloo Buergen ^b,
Wenqing Yao ^b, Yongfa Zhu ^{b,*}

^a Department of Chemistry, College of Environmental Science and Engineering, Nanjing University of Information Science & Technology, Nanjing 210044, P.R. China

^b Department of Chemistry, Tsinghua University, Beijing 100084, P.R. China

Received 7 March 2007; received in revised form 22 August 2007; accepted 19 October 2007
Available online 17 November 2007

Abstract

The novel hollow Mn_3O_4 -in- Co_3O_4 and hollow Co_3O_4 microspheres were prepared through a hydrothermal route, following by subsequent impregnation and annealing. The samples were characterized by SEM (EDS), TEM (ED), XRD, and N_2 adsorption. The chemiluminescence (CL) and catalytic properties for CO oxidation over these hollow samples were evaluated. The hollow Mn_3O_4 -in- Co_3O_4 catalyst showed a stronger CL response to CO and a higher catalytic activity for CO oxidation, compared with the hollow Co_3O_4 sample, which was attributed to the novel structure of crystals-in-ball.

© 2007 Elsevier B.V. All rights reserved.

Keywords: Hollow Mn_3O_4 -in- Co_3O_4 ; Hollow Co_3O_4 ; Chemiluminescence; CO oxidation

1. Introduction

Hollow structures with nano- to micrometers dimensions are an important class of materials due to their wide variety of potential applications, such as sensors, drug delivery carriers, artificial cells, acoustic insulators, fillers, light-weight structural materials, microreactors, catalysts/supports, adsorbents, etc. [1–5]. Template-directed synthesis represents an ideal approach to design the predetermined hollow structures. The commonly used templates include polystyrene latex, resin, silica, porous alumina, polymer gel, micelles/surfactant, and carbonaceous materials [6–13]. Recently, various carbon sources have been used to prepare other hollow materials [14–16]. It is well-known that the properties of materials are strongly dependent on

the morphology and structure of the particles. Hollow structures with microscales have many promising applications in catalysts carriers, microreactors or material storage; as a result, hollow microspheres have been a subject of extensive study [17,18]. For hollow nanospheres (typically less than 100 nm), however, it is difficult to encapsulate or accommodate large molecules (e.g. DNA, protein, etc.), due to their small sizes with available micromanipulation techniques. It is desirable to employ suitable colloidal templates to obtain relatively large hollow structures.

Herein, manganese-containing carbonaceous microspheres (MCMs) and pure carbonaceous microspheres (CMs) were synthesized by a simple hydrothermal method; and hollow Mn_3O_4 -in- Co_3O_4 microspheres (HMCMs) and hollow Co_3O_4 microspheres (HCMs) were prepared by the impregnation. The samples were characterized by scanning electron microscopy (SEM), energy disperse spectra (EDS), transmission electron microscopy (TEM), selected area electron diffraction (ED), X-ray diffraction (XRD), and N_2 adsorption. Chemiluminescence (CL) and catalytic

* Corresponding authors. Tel./fax: +86 25 5873 1090 (F. Teng), tel./fax: +86 10 6278 7601 (Y.F. Zhu).

E-mail addresses: tfwd@163.com (F. Teng), zhuyf@mail.tsinghua.edu.cn (Y.F. Zhu).

properties of the hollow samples were evaluated for CO oxidation. Importantly, the adopted approach is simple and environmentally friendly; and the obtained HMCMs could be potentially used for encapsulation of large guest molecules (e.g. DNA), which may be employed as advanced materials and biomaterials.

2. Results and discussion

2.1. Characterization of Mn_3O_4 -containing carbonaceous microspheres (MCMs)

The experiment section (preparation, characterization, evaluation of chemiluminescence properties and catalytic activity of the samples) is given in [supporting information](#).¹ Fig. 1a shows SEM images of MCMs. It can be observed that the uniformed MCMs have about 10 μm in size, and the surfaces of MCMs are smooth (the insert). However, TEM image of individual MCM reveals that the surface of MCM is not smooth virtually, but is coarse (Fig. 1b). This can be ascribed to the removal of residual organic compounds (i.e. oligosaccharides). The surfaces of MCMs became coarse due to the removal of these matters from the surface layer while MCMs were washed with water and alcohol. Li et al. [19] have reported that there are some nanopores in the surface layer, while they synthesized pure carbonaceous spheres. The existence of nanopores in surface layer is very important. These pores can not only increase the surface area, but also favor for the subsequent accommodation or adsorption of reactive species. ED patterns (the inset of Fig. 1b) of MCM fringe firmly confirm the formation of manganese oxides within MCM. All the observed diffraction rings can be indexed to a tetragonal structure of Mn_3O_4 nanocrystals (hausmannite). The presence of manganese within MCMs can be further confirmed by EDS spectra (see [supporting information of Fig. S1](#)). The formation of Mn_3O_4 within MCMs can be also supported by the observed phenomenon: while scanning MCMs sample with X-rays, the microspheres moved obviously due to the intrinsic magnetic properties of Mn_3O_4 . XRD patterns were further performed to determine the compositions of MCMs (Fig. 2a). The broad peak with low peak intensity centered at about $2\theta = 23.5^\circ$ can be indexed as [002] diffraction peak of turbostratic and polyaromatic carbonaceous materials. The broadening of the “graphite” peaks actually indicates the existence of highly disordered structures in the product. On the other hand, no other diffraction peaks can be observed from XRD patterns. It is probably that the formed Mn_3O_4 nanocrystals are too small to be detected by XRD, since the aggregation or growth of Mn_3O_4 nanocrystals may be significantly refrained by the net of carbonaceous materials.

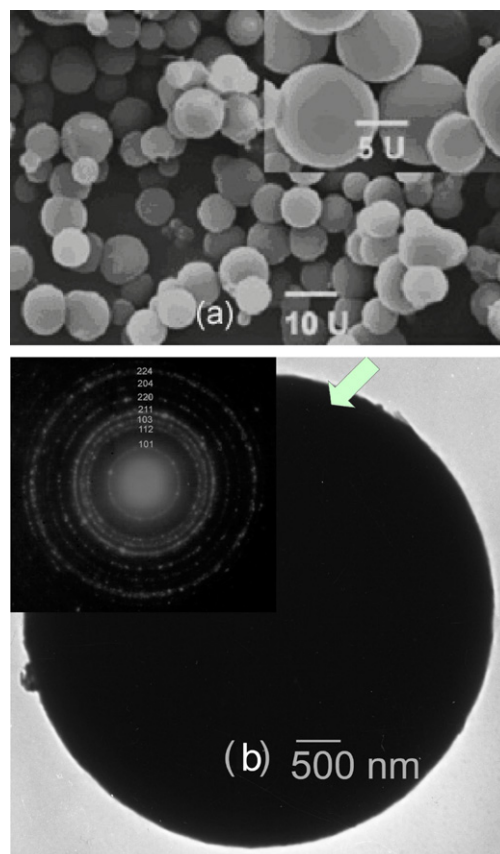


Fig. 1. SEM (a) and TEM micrographs (the insert of ED for fringe region) (b) of manganese-containing carbonaceous microspheres (MCMs).

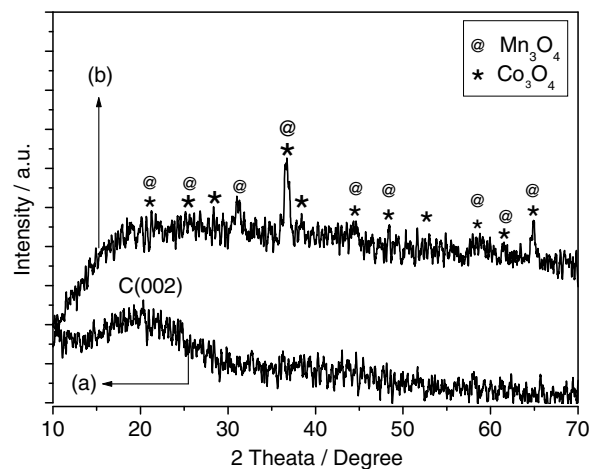


Fig. 2. XRD patterns of the samples: (a) manganese-containing carbonaceous microspheres (MCMs); (b) hollow Mn_3O_4 -in- Co_3O_4 microspheres (HMCMs).

2.2. Characterization of Hollow Mn_3O_4 -in- Co_3O_4 microspheres (HMCMs)

Fig. 2b shows XRD patterns of HMCMs after being annealed at $450^\circ C$ for 2 h. The sample was composed of Mn_3O_4 and Co_3O_4 nanocrystals. γ - Mn_3O_4 can be indexed to a tetragonal structure with the lattice constants

¹ This material is available free of charge via the Internet at <http://elsevier.com>.

$a = 0.5762$ nm and $c = 0.9469$ nm, which agree well with the values reported in the literature (JCPDS Card. No. 24-0734). Co_3O_4 nanocrystals show a spinel structure with the lattice constants $a_0 = 0.8084$ nm (space group of Co_3O_4 : $\text{Fd}3\text{m}$, JCPDS file no. 43-1003). Moreover, no significant orientation can be seen from the XRD patterns due to the random arrangement of different nanocrystals. As far as the formation of the low-valence oxides is concerned, we assume that the surface functional groups (OH) can impart the reduction ability to MCMs that can reduce metal ions into lower valence ion or metallic elements. Such reduction ability has been reported in the literatures [20–22].

Fig. 3a and b presents the typical SEM micrographs of HMCMs. It reveals that the sizes of HMCMs are about $5 \mu\text{m}$, significantly smaller than those ($10 \mu\text{m}$) of the solid MCMs templates. It is obvious that HMCMs retained the morphological characteristics of the original MCMs templates except for shrinkage in size (about 50%). It is easily understood that upon drying and annealing, the dehydration and dehydroxylation may lead to the contraction of the sample. As a result, the rough surface coatings were constructed by randomly aggregated Co_3O_4 nanocrystals. A few broken microspheres strongly confirm that the formation of hollow structures truly, with the walls of about 250 nm in thickness. Since the diameters of the original MCMs templates are much larger than the thickness of Co_3O_4 coating, a few microspheres collapsed during annealing. The EDS spectra of HMCMs firmly confirm the presence of both manganese and cobalt (the atomic ratio of Co to Mn is 1.5:1) (see supporting information

of Fig. S2). Further, the surface microstructure of individual HMCM was scanned by high-magnification SEM. Fig. 3c reveals clearly that HMCMs have the hollow interior of about $4.5 \mu\text{m}$ in size and the shell of about 250 nm in thickness. Fig. 3d reveals that HMCMs have a crinkle-like surface structure, which is different from that of MCMs templates. This can be ascribed to the fact that the walls are comparably flimsy, easy to curl and shrink while the templates are removed. Most interestingly, Fig. 3e and f reveal that there are some holes on the surface of the shell, which may be caused by the prompt release of vapor or CO_2 gases due to the combustion of carbonaceous chemicals. Fig. 3g and h obviously reveals that there are some cores of Mn_3O_4 crystals in one ball. The core may form from the “loose” aggregate of Mn_3O_4 nanocrystals, which is not a hard agglomerate. As we know, Mn_3O_4 nanocrystals were originally trapped within the carbonaceous mist after hydrothermal treatment; Mn_3O_4 nanocrystals were protected from growth or agglomeration with carbonaceous mist. As a result, Mn_3O_4 nanocrystals may form the soft aggregates, not hard aggregates [23].

HMCMs were further characterized by TEM. The clair-obscure contrast between the inner and the outer regions of the ball can be observed clearly, revealing the presence of hollow interior. It can be also observed that some balls contain a few aggregates of Mn_3O_4 , but others contain only one (Fig. 4a). ED patterns of the sample (Fig. 4b) further demonstrate that Mn_3O_4 nanocrystals were contained in the sample. Moreover, the clair-obscure contrast in individual core suggests that the core resulted from the aggregates

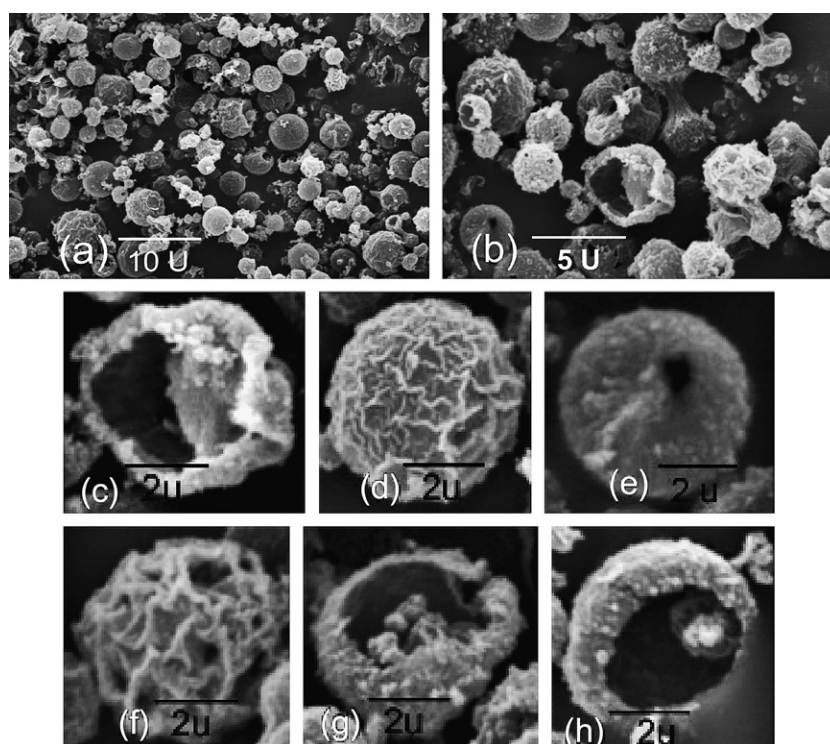


Fig. 3. SEM micrographs of hollow Mn_3O_4 -in- Co_3O_4 microspheres (HMCMs): (a, b) low magnification, (c–h) high-magnification.

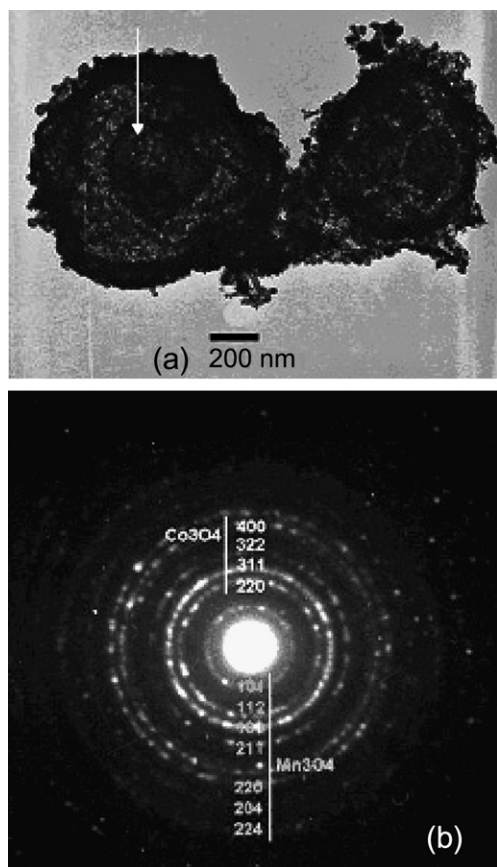


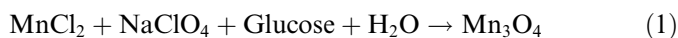
Fig. 4. TEM micrographs (a) and ED patterns (b) of hollow Mn_3O_4 -in- Co_3O_4 microspheres (HMCMs).

of Mn_3O_4 nanocrystals. Interestingly, the shell resulted from Co_3O_4 nanocrystals, which spontaneously packed to form a porous wall. The result is different from the reports [24,25]. Therefore, it is reasonable to believe that the wall may have the porous structure; that the wall was uneven and some pores connected to the inner hollow channel in surface layer, which favor for the access of foreign reacting molecules.

2.3. Formation of MCMs and HMCMs

Pure carbonaceous microspheres are first prepared by dehydration of saccharide under hydrothermal conditions [26]. It has been reported that under hydrothermal conditions, a variety of chemical reactions for glucose could take place, which resulted in a complex mixture of organic compounds [27]. As a result, it is difficult to determine exactly the chemical reactions in the sealed autoclave. In our experiment, after hydrothermal treatment, the appearance of black solids and the increased viscosity of the resulting solution indicated that some aromatic compounds and oligosaccharides may have formed, which has been denoted a “polymerization” process [26]. The carbonization step may arise from the cross-linking process of oligosaccharides or other macromolecules. The formation of MCMs seems to conform to the LaMer model [28]. While the solution reached a critical supersaturation, a short burst of nucle-

ation occurred. The resulting nuclei then grew uniformly through the diffusion of solutes toward the nuclei surfaces until the final size was attained. In our experiment, the chemical reaction below may have taken place:



In this process, NaClO_4 , a typical oxidant, would oxidize Mn(II) to Mn(IV) [29]. However, since the hydroxyls of glucose can reduce Mn(IV) to Mn(II) or/and Mn(III) ; as a result, Mn_3O_4 formed under hydrothermal conditions. Importantly, in comparison to the synthesis of polymer spheres, the adopted approach has two outstanding features: (i) the synthetic approach is very simple since no intricate operations are involved; (ii) the approach is environmentally friendly, since no toxic reagents were used. Therefore, the as-prepared microspheres could potentially be used in biodiagnostics. For preparation of polymer microspheres, however, toxic reagents (organic solvents, initiators or/and surfactants) are commonly used.

Basing on the report by Li et al. [30], the surfaces of MCMs are hydrophilic due to the functional groups (OH , C=O), and the surface layer contains the nanopores. We assumed that the functionalized surface layers of MCMs, acting a host, could adsorb or accommodate cobalt ions, leading to the formation of a guest coating. This may be through electrostatic or chelating interactions between foreign metal ions and surface functional groups (OH , C=O) [31]. Further, a sol–gel process (i.e. noncrystalline process) is involved in the formation of cobalt oxide due to the chelating effect of surface functional groups [9]. Subsequently, upon drying and annealing, the guest coating can be further solidified and condensed. The annealing treatment in air can not only remove the carbonaceous templates, but also give rise to the self-supporting cobalt oxide nanocrystals.

2.4. The CL and catalytic properties over the catalysts

2.4.1. The CL response to CO over the catalysts

CL spectra were used to quantitatively analyze the given catalytic oxidation reaction. The temperature dependence on the (CL) intensity of HMCMs was investigated (see supporting information of Fig. S3). The results showed that the CL intensities of HMCMs increased with the temperature. It is easily understood that more CO molecules were oxidized into CO_2 molecules at high temperatures. Hollow Co_3O_4 microspheres (HCMs) without Mn_3O_4 cores were also prepared in order to compare with HMCMs (see supporting information of Fig. S4). Fig. 5 shows the CL spectra of HMCMs and HCMs at 180 °C. The CL intensity response to CO of HMCMs is much higher than that of HCMs, indicating that more CO molecules were oxidized into CO_2 molecules. When CO molecules were oxidized catalytically to form CO_2 molecules on the surface of the catalyst, an amount of energy was released, which would be absorbed by some CO_2 molecules. As a result, CO_2 molecules would jump from ground state up to excited state.

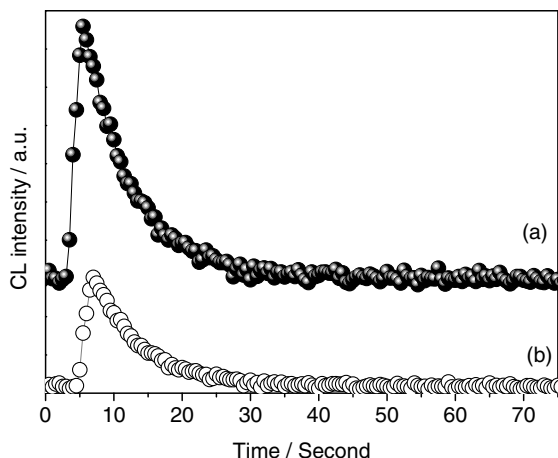


Fig. 5. The chemiluminescence (CL) profiles response to CO of (a) hollow Mn_3O_4 -in- Co_3O_4 microspheres (HMCs) and (b) hollow Co_3O_4 microspheres (HMs): Flow rate of the gas mixture of air and CO: 200 mL min^{-1} ; CO concentration: $200 \mu\text{g mL}^{-1}$; Measure temperature: 180°C .

While CO_2 molecules decayed from the excited state to the ground state, a weak light would be emitted. The CL intensity of the emitted light varies linearly with the produced CO_2 concentration; therefore, the CL spectrum response to CO is as an effective means to evaluate CO oxidation over the catalysts [32]. The results above may also mean that HMCs had a higher catalytic activity for CO oxidation than HMs. The catalytic activity for CO oxidation over HMCs was further evaluated.

2.4.2. The catalytic activity for CO oxidation over the catalysts

Fig. 6 shows the activities for CO oxidation over HMCs and HMs. The complete oxidation of CO over HMCs and HMs was achieved at 150°C and 230°C , respectively. The catalytic activity of HMCs is significantly higher than that of the latter, which is well consistent with their CL order. The textural properties of HMCs

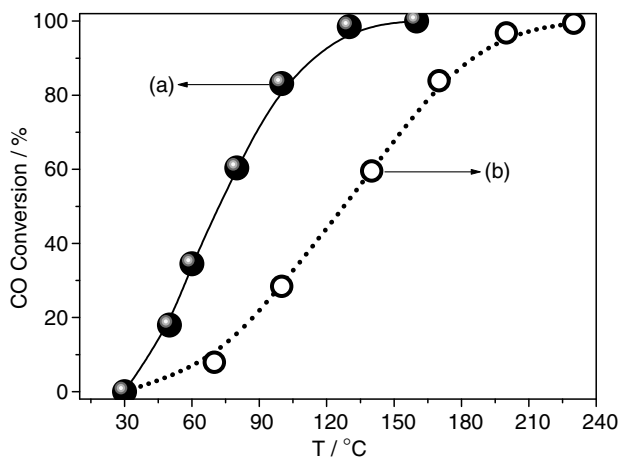


Fig. 6. The activities of CO oxidation over (a) hollow Mn_3O_4 -in- Co_3O_4 microspheres (HMCs) and (b) hollow Co_3O_4 microspheres (HMs): 2 vol.% CO, 98 vol.% air, gas hourly space velocity (GHSV) = $12,000 \text{ h}^{-1}$.

were characterized by N_2 adsorption isotherm. The BET surface area ($31.6 \text{ m}^2 \text{ g}^{-1}$) of HMCs is significantly larger than that (ca. $1.5 \text{ m}^2 \text{ g}^{-1}$) of the hollow microspheres with an outer diameter of $5 \mu\text{m}$ and an inner diameter of $4.5 \mu\text{m}$. The surface area of the latter is calculated on base of idea hollow microspheres (the theory density (F) of Co_3O_4 is 6.056 g cm^{-3}). The calculation result further confirms that the increased surface area (ca. $30 \text{ m}^2 \text{ g}^{-1}$) of HMCs may result from the pores in wall. The porous structure of MCMs templates was passed onto the resultant wall and formed the reverse copy products after removal of the carbonaceous template. The increase of surface areas supports the generation of the pore structure. The porous wall structure of of this sample may generate from a closely packing of Co_3O_4 nanocrystals. Thus, the sample has two kinds of pores, which is composed of large hollow interiors and small pores in wall [33]. It is important that these interconnected pore networks would favor for molecule accessibility to the active surface of the nanocrystals and mass transport when the materials was used as catalyst or microreactor, because gases and liquids can enter the nanopores and the inner chambers of the hollow spheres.

The BET surface areas of HMCs and HMs are 31.6 and $30.7 \text{ m}^2 \text{ g}^{-1}$, respectively. Considering their similar surface areas, the activity difference may be closely related to their different microstructures. The higher activity of HMCs could result from the contribution of Mn_3O_4 nanocrystals within Co_3O_4 shell. The reacting gases (CO and air) can fluently pass through the wall and get access to the surface of Mn_3O_4 nanocrystals within the interior of HMCs. Manganese and cobalt oxides are important catalysts for CO oxidation due to their outstanding structural flexibility and novel physicochemical properties [26,34,35], the high activity of HMCs could result from a synergetic effect of Mn_3O_4 and Co_3O_4 .

3. Summary

Mn_3O_4 nanocrystals could be encapsulated in hollow Co_3O_4 microspheres by a simple method. The hollow Mn_3O_4 -in- Co_3O_4 microspheres showed a stronger CL intensity and a higher catalytic activity for CO oxidation than the hollow Co_3O_4 ones, which were attributed to the novel microstructure of crystals-in-ball.

Acknowledgements

This work is financially supported by Chinese Postdoctoral Science Foundation (Grant 20060390057) and Chinese National Science Foundation (Nos. 20433010, and 20571047).

Appendix A. Supplementary material

Supplementary data associated with this article can be found, in the online version, at doi:10.1016/j.catcom.2007.10.032.

References

- [1] F. Caruso, R.A. Caruso, *Science* 282 (1998) 1111.
- [2] Y. Sun, B. Mayers, Y. Xia, *Adv. Mater.* 15 (2003) 641.
- [3] S.-W. Kim, M. Kim, W.Y. Lee, T. Hyeon, *J. Am. Chem. Soc.* 124 (2002) 7642.
- [4] Y. Yin, R.M. Rioux, C.K. Erdonmez, S. Hughes, G.A. Somorjai, A.P. Alivisatos, *Science* 304 (2004) 711.
- [5] J. Yang, L. Qi, C. Lu, J. Ma, H. Cheng, *Angew. Chem. Int. Ed.* 44 (2005) 598.
- [6] R.A. Caruso, *Angew. Chem. Int. Ed.* 43 (2004) 2746.
- [7] P.J. Brusinsma, A.Y. Kim, J. Liu, S. Baskaran, *Chem. Mater.* 9 (1997) 2507.
- [8] S.A. Davis, S.L. Burkett, N.H. Mendelson, S. Mann, *Nature* 101 (1997) 385.
- [9] J. Huang, T. Kunitake, *J. Am. Chem. Soc.* 125 (2003) 11834.
- [10] D.G. Shchukin, J.H. Schattka, M. Antonietti, R.A. Caruso, *J. Phys. Chem. B* 107 (2003) 952.
- [11] F. Schüth, *Angew. Chem. Int. Ed.* 42 (2003) 3604.
- [12] Y. Tao, H. Kano, K. Kaneko, *J. Am. Chem. Soc.* 125 (2003) 6044.
- [13] S. Lee, W.M. Sigmund, *Chem. Commun.* 6 (2003) 780.
- [14] S.H. Joo, S.J. Choi, I. Oh, J. Kwak, Z. Liu, O. Terasaki, R. Ryoo, *Nature* 412 (2001) 169.
- [15] T.W. Kim, I.S. Park, R. Ryoo, *Angew. Chem. Int. Ed.* 42 (2003) 4375.
- [16] M.-M. Titirici, M. Antonietti, A. Thomas, *Chem. Mater.* 18 (2006) 3808.
- [17] Z.L. Wang, J.S. Yin, *Chemphys. Lett.* 289 (1998) 189.
- [18] J.W. Liu, W.J. Lin, X.Y. Chen, S.Y. Zhang, F.Q. Li, Y.T. Qian, *Carbon* 42 (2004) 669.
- [19] J. Cho, Y.J. Kim, T.J. Kim, B. Park, *Angew. Chem. Int. Ed.* 40 (2001) 3367.
- [20] I. Ichinose, T. Kawakami, T. Kunitake, *Adv. Mater.* 10 (1998) 535.
- [21] S. Chen, H. Zeng, *Carbon* 41 (2003) 1265.
- [22] R. Fu, H. Zeng, Y. Lu, *Carbon* 31 (1993) 1089.
- [23] B. Liu, H.C. Zeng, *Small* 1 (2005) 566.
- [24] W. Wang, C. Xu, G. Wang, Y. Liu, C. Zheng, *Adv. Mater.* 14 (2002) 837.
- [25] J. Wang, J. Sun, Y. Bao, X. Bian, *J. Mater. Sci. Technol.* 19 (2003) 489.
- [26] Y.F. Shen, P.R. Zenger, N.R. DeGuzman, L.S. Suib, L. McCurdy, I.D. Potter, C.L. O'Young, *Science* 260 (1993) 511.
- [27] X. Sun, Y. Li, *Angew. Chem. Int. Ed.* 43 (2004) 597.
- [28] T. Sakaki, M. Shibata, T. Miki, H. Hirose, N. Hayashi, *Biores. Technol.* 58 (1996) 197.
- [29] V.K. Lamer, *Ind. Eng. Chem.* 44 (1952) 1270.
- [30] Y.-S. Ding, X.-F. Shen, S. Gomez, H. Luo, M. Aindow, Steven L. Suib, *Adv. Funct. Mater.* 16 (2006) 549.
- [31] X. Sun, J. Liu, Y. Li, *Chem. Eur. J.* 12 (2006) 2039.
- [32] Y. Zhu, J. Shi, Z. Zhang, C. Zhang, X. Zhang, *Anal. Chem.* 74 (2002) 120.
- [33] G.S. Chai, S.B. Yoon, J. Ho Kim, J.-S. Yu, *Chem. Commun.* 11 (2004) 2766.
- [34] M. Yin, S. O'Brien, *J. Am. Soc. Chem.* 125 (2003) 10180.
- [35] W.S. Seo, H.H. Jo, K. Lee, B. Kim, S.J. Oh, J.T. Park, *Angew. Chem. Int. Ed.* 43 (2004) 1115.